ResearchGate

See discussions, stats, and author profiles for this publication at: https://www.researchgate.net/publication/243568445

Heavy Fermion Superconductivity and Antiferromagnetic Ordering in CePt3Si without Inversion Symmetry

Article *in* Journal of the Physical Society of Japan · April 2007

DOI: 10.1143/JPSJ.76.051009

CITATIONS
69

READS
211

8 authors, including:

Ernst Bauer
TU Wien
614 PUBLICATIONS **9,842** CITATIONS
SEE PROFILE

Andrey Prokofiev
TU Wien
157 PUBLICATIONS **3,598** CITATIONS
SEE PROFILE

Alex Amato
Paul Scherrer Institut
518 PUBLICATIONS **10,875** CITATIONS
SEE PROFILE

Werner Bramer-Escamilla
Yachay Tech.
28 PUBLICATIONS **407** CITATIONS
SEE PROFILE

Some of the authors of this publication are also working on these related projects:

Chemical pressure in FeSe superconductors View project

Thermoelectric cage compounds: a combined experimental and ab-initio effort View project

All content following this page was uploaded by Ismardo J Bonalde on 18 March 2014.

The user has requested enhancement of the downloaded file.

Heavy Fermion Superconductivity and Antiferromagnetic Ordering in $CePt_3Si$ without Inversion Symmetry

E. BAUER[1]*, H. KALDARAR[1], A. PROKOFIEV[1], E. ROYANIAN[1], A. AMATO[2], J. SEREN[3], W. BRÄMER-ESCAMILLA[4] and I. BONALDE[4]

[1]*Institute of Solid State Physics, Vienna University of Technology, A-1040 Wien, Austria*
[2]*Laboratory for Muon-Spin Spectroscopy, Paul Scherrer Institute, CH-5232 Villigen PSI, Switzerland*
[3]*Lab. Bajas Temperaturas, Centro Atómico Bariloche (CNEA) 8400 S.C. de Bariloche, Argentina*
[4]*Centro de Física, Instituto Venezolano de Investigaciones Científicas, Apartado 21874, Caracas 1020-A, Venezuela*

Heavy fermion superconductivity in absence of inversion symmetry of the crystal structure is basically controlled by a Rashba-like antisymmetric spin orbit coupling which splits the Fermi surface and removes the spin degeneracy of electrons. The Fermi surface splitting originates a mixing of spin-singlet and spin-triplet states in the superconducting condensate. Such constraints are responsible for various uncommon features of the superconducting ground state and are discussed here in view of $CePt_3Si$, the first heavy fermion superconductor missing a centre of symmetry. We recall and discuss normal and superconducting properties of $CePt_3Si$ and relate them to recently developed phenomenological theories.

KEYWORDS: $CePt_3Si$, superconductivity, long range magnetic order

1. Introduction

Since the discovery of superconductivity almost 100 years ago, countless observations have been made with relevance to practical applications as well as with respect to its fundamental understanding as a macroscopic quantum mechanical phenomenon. For the vast majority of materials, superconductivity turned out to be related to Cooper pairs mediated by electron - phonon interaction. The retardation effect associated with the electron - phonon interaction [$\propto W/(\hbar\omega_D)$, W ... electronic band width, ω_D ... Debye frequency] appears to be sufficient for ordinary s, p and d systems with large bandwidths, additionally favoured for pretty soft crystals with low Debye temperatures.[1] This type of interaction generally results in the symmetric s-wave state of the Cooper pairs, where the total spin and orbital momenta are zero. The antisymmetric spin state of the two electrons forming the Cooper pair, $\vec{s} = 0$, requires a symmetric orbital momentum $\vec{l} = 0$ to keep the total wave function antisymmetric. Highly symmetric s-wave superconductivity is characterised by a gap function ψ, which does not have any nodal structure, i.e., the gap in the electronic density of states does nowhere vanish around the Fermi surface. Consequently, physical properties like the specific heat, the NMR relaxation rate or the thermal conductivity exhibit an activation type of behaviour, primarily determined from the gap width of the system. In symmetric s-wave superconducting states only the gauge symmetry is broken, and all materials which are accounted for in this framework are termed *conventional superconductors*.

More than two decades ago, however, the magnetic intermetallic compound $CeCu_2Si_2$ was found to undergo a transition into a superconducting ground state around 0.7 K,[2] while isostructural and nonmagnetic $LaCu_2Si_2$ remains in its normal state down to the lowest temperatures. Many of the superconducting properties and parameters of $CeCu_2Si_2$ did not straightforwardly comply with the BCS theory, well established to describe the physics of conventional superconductors. One of the exceptional features in $CeCu_2Si_2$ is the fact that heavy quasiparticles condenses into heavy Cooper pairs, carrying the supercurrent. Heavy quasiparticles in this cerium compound are formed by Kondo type interactions and are a result of the loss of spin degrees of freedom because of the tendency of the Kondo effect to form a nonmagnetic ground state. This compound, together with the large family of high T_c superconductors - which will not be discussed here - discovered few years later triggered intense research on a steady growing group of superconducting materials, known as *unconventional superconductors*. In such superconductors the time reversal and/or a crystallographic point group symmetry is broken in addition to the gauge symmetry. The majority of these materials is found to hold nodes in the electronic density of states, so that the gap created due to the formation of Cooper pairs vanishes, at least partly, e.g., along lines or points at the Fermi surface. Consequently, physical quantities are no longer characterised by exponential temperature dependences, rather, simple power laws may be observed instead.

In contrast to simple metals showing superconductivity, in materials with strong electron correlations Cooper pairs may be formed not by the interaction of electrons with phonons, but rather by magnetic fluctuations. Theoretically, this can be ascribed to narrow electronic bands, inherent to highly correlated electron systems. As a consequence, the effective mass m^* of the charge carriers becomes very large ($m^* \approx 10$ to $1000 \times m_0$, m_0 ... free electron mass), thus the particle velocity is small. The retardation effect, $W/\hbar\omega_D$, weakens because of the small bandwidth W. Heavy fermion compounds naturally provide alternative possibilities for attractive forces between electrons, i.e, spin fluctuations, since many of such sys-

*E-mail address: bauer@ifp.tuwien.ac.at

tems exhibit weak magnetic order or are in the proximity to a magnetic instability. Applying control parameters like pressure or substitution allows to tune these materials across a quantum critical point, where frequently superconductivity occurs and Cooper pairs are, most likely, formed by magnetic fluctuations.[3] Cooper pairing in such a scenario may happen also in a different angular momentum channel. This means that Cooper pairs may have either spin singlet or spin triplet configurations and the orbital angular momentum $\vec{l} > 0$ may lead to a highly anisotropic gap with lines or points as zero nodes. Since the Cooper pairs consist of heavy particles, the upper critical field H_{c2} becomes exceptionally large.

Ce-based heavy fermion superconductors, however, are still few in numbers, adduced by prototypic $CeCu_2Si_2$.[2] The application of pressure in the 10 to 30 kbar range to members of this structure family such as $CeCu_2Ge_2$,[4] $CePd_2Si_2$[5] and $CeRh_2Si_2$[6] is sufficient to trigger superconductivity as well. Few years ago, a new family of cerium compounds, $CeMIn_5$, was added where at ambient pressure heavy fermion superconductivity occurs for M = Co and Ir at T_c = 2.3 and 0.4 K, respectively.[7,8] Again, pressure initiates superconductivity, e.g., in $CeRhIn_5$ below $T_c^{max} = 2.1$ K.[9] The crystal structure of these latter compounds can be considered quasi-two-dimensional variants of $CeIn_3$ ($AuCu_3$-type). Cubic $CeIn_3$ becomes superconducting at $\sim$25 kbar.[3]

It is a general presumption that time reversal invariance provides the necessary conditions for spin-singlet Cooper pairing, while spin-triplet pairing needs additionally inversion symmetry.[10] The missing of a centre of inversion should thus be disadvantageous in forming a spin-triplet condensate. As parity is not a symmetry in non-centrosymmetric systems, spin singlet and spin triplet cannot be distinguished anymore.

Superconductors without inversion symmetry were investigated in previous years, but not much care was taken to the fact that the crystal symmetry misses inversion. Among them are binary R_2C_{3-y} with R = La or Y, which can be substituted by various other elements. Superconducting transition temperatures in the 10 to 20 K range were observed with $T_c = 18$ K found for Y_2C_3.[12–14] The transition temperature, however, profoundly depends on small changes of the lattice parameters.[14] Elements constituting these materials are lightweight, causing, most likely, only minor spin-orbit coupling. Another example is $Cd_2Re_2O_7$ with T_c = 1 K.[15,16] Although the pyrochlore structure of $Cd_2Re_2O_7$ exhibits a centre of symmetry, a series of low temperature structural phase transitions provokes superconductivity to occur in a non-inversion symmetric environment. Different to the previous case, strong spin-orbit coupling dramatically affects the electronic band structure. Nevertheless, normal state properties of these systems are quite simple and the charge carriers do no exhibit large effective masses. Interesting physics was found in recently discovered $Li_2(Pd,Pt)_3B$.[17,18] Li_2Pd_3B is accounted for in terms of a conventional BCS-like superconductor; however, various features in Li_2Pt_3B refer to unconventionality.[18–20] An asset of the latter systems is the chance of a continuous substitution of Pd/Pt without destroying superconductivity.[18]

Also well known, amorphous superconductors do not exhibit a centre of inversion. The diffusivity of these materials is very low in comparison to that of crystalline metals and alloys. The resulting Ginzburg-Landau Parameter κ is thus very large ($\kappa \gg 1$), making these materials examples of superconductors in the "very dirty limit". Additionally, because of the low diffusivity, $H_{c2}(0)$ becomes large.[21]

Theoretically, superconductivity in systems without inversion symmetry was considered mostly in the context of surfaces and films.[22]

All previously studied superconductors with strong electron correlations in the normal state region are characterised by a centre of inversion in its crystal structure. This makes it possible to separately consider the even (spin-singlet) and odd (spin-triplet) components of the superconducting order parameter. The first examples of heavy fermion superconductivity (HFSC) without inversion symmetry were discovered only recently.[23] Members of this family, which have been reported so far are $CePt_3Si$,[23] UIr,[24] $CeRhSi_3$,[25] and $CeIrSi_3$.[26] Whereas $CePt_3Si$ shows superconductivity already at ambient pressure, a transition into a superconducting ground state was found for the remaining ones only at applied hydrostatic pressure of the order of 10 to 20 kbar.

Various intriguing observations were made in the case of $CePt_3Si$: i) Superconductivity (T_c = 0.75 K) is mediated by Cooper pairs formed by heavy quasiparticles due to the presence of Kondo interactions; ii) Long range magnetic order (T_N = 2.2 K) coexists with superconductivity on a microscopic scale. The coupling between both phenomena, however, turns out to be quite weak. iii) The upper critical field $H_{c2}(0) \approx 4$ T exceeds the Pauli-Clogston limit ($H_P \approx 1.1$ T) by far and the anisotropy of $H_{c2}^{\parallel}$ and $H_{c2}^{\perp}$ is very small. iv) The $1/T_1$ relaxation rate of NMR measurements does not follow the simple T^3 power law of HFSC and additionally exhibits a Hebel-Slichter peak below T_c. The latter has never been observed in HFSC and may refer to, at least, a s-wave component in the SC order parameter. v) penetration depth measurements and thermal conductivity,[27,28] as well as specific heat[29] performed on $CePt_3Si$ at very low temperatures reveal power laws, indicating line nodes in the electronic gap. The absence of paramagnetic limiting would favour spin triplet pairing, in contradiction to the absence of inversion symmetry. The Hebel-Slichter peak, on the one hand, is a fingerprint of conventional superconductivity, but power laws in thermodynamical properties are archetypal of unconventional features in superconductivity. Various physical quantities, characterising $CePt_3Si$ both in the normal and in the superconducting state are summarised in Table 1.

These observations have triggered substantial theoretical work on the role of pairing symmetry in such superconductors. The essential element to model non-centrosymmetric systems is the presence of antisymmetric spin-orbit coupling. An inherent feature is then the mixing of spin-singlet and spin-triplet Cooper-pairing channels which are otherwise distinguished by parity.[11]

Table I. Normal state and superconducting properties of $CePt_3Si$. Data are collected from Ref. 23 if not separately indicated.

$CePt_3Si$	
crystal structure	tetragonal
space group	$P4mm$
lattice parameter	$a = 0.4072(1)$ nm
	$c = 0.5442(1)$ nm
Sommerfeld value of specific heat	$\gamma_n \approx 0.39$ J/molK^2
magnetic phase transition temperature	$T_N = 2.25$ K
magnetic propagation vector[46]	$\vec{q} = (0, 0, 1/2)$
ordered moment[46]	$\mu_s \approx 0.15\ \mu_B$
superconducting transition temperature	$T_c = 0.75$ K
upper critical field	$H_{c2}(0) \approx 4$ T
slope of upper critical field	$H'_{c2} = -8.5$ T/K
thermodynamic critical field	$\mu_0 H_c(0) = 26(2)$ mT
correlation length	$\xi = 8.1$ nm
Ginzburg Landau parameter	$\kappa_{GL} = H_{c2}(0)/(\sqrt{H_c}) \approx 140$
London penetration depth	$\lambda = \kappa \cdot \xi \approx\ 1.1\mu$m
nodal structure[27–29]	line-nodes

This mixing of pairing states, yielding a two-component order parameter, seems to be the appropriate scenario to account for the above indicated, mutually contradicting, experimental features observed in ternary $CePt_3Si$.

Not only superconductivity is of interest in this system, rather, the paramagnetic properties, dominated by crystalline electric field (CEF) splitting and the Kondo effect, are interesting subjects by themself. In the present work we show how the major interaction mechanisms present in normal state $CePt_3Si$ can be understood and disentangled by a dilution of Ce/La and by pressure and magnetic fields; and how substitutions influences the balance of magnetic order and superconductivity. The superconducting state is reviewed and discussed in terms of recently developed theoretical models. Also, sample dependent properties, prominent for $CePt_3Si$, are discussed.

2. Crystal structure and sample dependent properties

An isothermal section of the Ce-Pt-Si phase diagram at 600° C was compiled by Gribanov et al.[30] They pointed out that the interaction of Ce, Pt and Si leads to the formation of at least nine stable ternary phases. Except for Ce_3Pt_4 all binaries of the Ce-Pt and Ce-Si systems extends into the ternary area. Seven of these ternary systems are expected to have a fixed composition, while the remaining $CePt_2Si_2$ and $Ce(Pt,Si)_2$ show a homogeneity range of up to 7 %. It is interesting to note that binary compounds in the Pt-Si system do not dissolve cerium. A binary compound $CePt_3$ is missing, however, $CePt_2$ has an extraordinarily broad homogeneity region, it dissolves Pt up to a composition $Ce_{25}Pt_{75}$.[30]

$CePt_3Si$ is the first member of the silicide RET_3Si family (RE = rare earth, T = transition metal). It crystallizes in a tetragonal crystal structure with space group $P4mm$ (No. 99),[31] isotypic with the ternary boride $CePt_3B$.[32] Crystallographic data are listed in Table 1. The melting temperature is about 1390 °C.[31]

In the $CePt_3Si$ structure, see Fig. 1, each cerium ion has 16 nearest neighbors, 12 platinum and 4 silicon atoms $[Pt_{12}Si_4]$. Pt1 is in the center of distorted trigonal prism

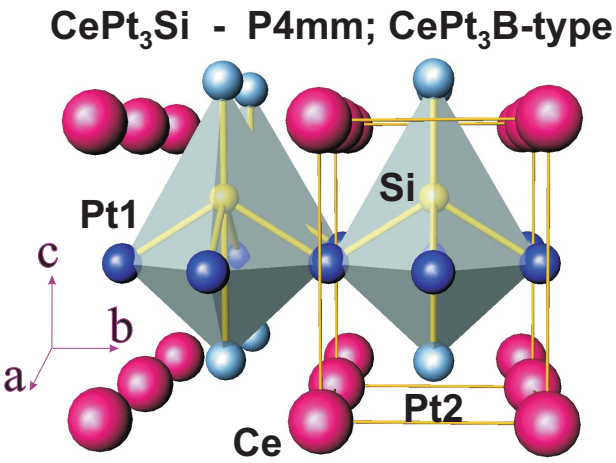

Fig. 1. Crystal structure of $CePt_3Si$. The bonds indicate the pyramidal coordination $[Pt_5]Si$ around the Si atom.

with three additional atoms (two Pt and one Si atom), which cap the tetra-angular faces of the prism $[Ce_4Pt_4Si]$. The Pt2 atom is coordinated by a distorted tetragonal prism of six platinum and two silicon atoms $[Pt_6Si_2]$. The coordination polyhedron of Si atoms is a tetragonal pyramid of five platinum atoms.[31] The space group $P4mm$ refers to the fact that a mirror plane perpendicular to the $\vec{c}$-axis is missing, responsible for the absence of inversion symmetry. This fact can easily be read-off from the crystal structure sketched in Fig. 1.

Physical properties of $CePt_3Si$ have already been studied by different groups on samples prepared with various techniques. The initial method used was argon arc melting revealing the standard set of data for $CePt_3Si$, i.e., $T_N = 2.25$ K and $T_c = 0.75$ K.[23] Material prepared by high frequency melting yielded about the same characteristics. Depending on the particular heat treatment of the samples, a further phase transition in the superconducting state was identified,[33] where the second phase transition shows a distinct dependence of the upper critical field. Specific heat studies carried out by Kim et al.[34]

also unambiguously revealed a second phase transition in the superconducting state at $T < 0.48$ K in nominally $CePt_3Si$ samples with $T_c = 0.75$ K, which was found to be due to a second phase of $Ce_3Pt_{23}Si_{11}$. This double transition structure became even more accentuated by a Ce deficiency in $Ce_{1-x}Pt_3Si$, and is reproducible for $x \geq 2$ %. Very recently, Nakatsuji et al.[35] found for a heat-treated nominal $CePt_3Si$ single crystalline material direct evidence for a double superconducting transition from heat capacity and magnetic susceptibility measurements.

Motoyama et al.[36] carried out very detailed studies concerning slight off-stoichiometries on the Ce, Pt and Si sites of $CePt_3Si$ and on the effect of different heat treatments. They found that the most pronounced antiferromagnetic transition occurs in the almost nominal $CePt_3Si$. Anomalies were observed upon variations in composition. A ferromagnetic anomaly was identified at 3.0 K for Pt-rich samples, while an antiferromagnetic anomaly was found at 4.0 K in Pt-poor samples. Superconductivity appears to be suppressed by the ferromagnetic phase. On the other hand, Ishikawa et al.[37] reported that superconductivity in $CePt_3Si$ coexists with incipient electric-multipolar order instead of the more simple antiferromagnetic state.

A remarkable observation was made previously by Tackeuchi et al.[29] in single crystalline $CePt_3Si$. They found from specific heat measurements a very sharp magnetic phase transition at $T_N = 2.25$ K, but the superconducting phase transition temperature is as low as 0.45 K. The quality of this single crystal may follow from a low residual electronic specific heat coefficient in the superconducting state, $\gamma_s = 34$ mJ/molK^2, but residual resistivity data have not been reported so far.

To illustrate some of the sample dependent properties of $CePt_3Si$, we refer to recently performed penetrations depth studies carried out on two single crystals from different batches. Self-evident results are depicted in Fig. 2. The penetration depth data of single crystal #2 shows a much wider transition than both single crystal #1 and polycrystalline material.[67] This results, along with those found from specific heat measurements, suggests that sample-related effects could be a principal cause of the unusual behaviours observed in $CePt_3Si$. Stoichiometric analyses, using an electron microprobe technique, of the two single crystals used in the penetration depth measurements indicated the presence of a spurious second phase in the single crystals studied.[67] The response of $\lambda(T)$ below T_c in crystal #2, with high content of Si in the secondary phase, may be associated with an antiferromagnetic transition at 0.48 K, as suggested by Kim et al. We note that $\lambda(T)$ in crystal #2 drops sharply around 0.45 K, whereas in crystal #1 and in the polycrystalline sample such a drop is smoother and occurs around 0.53 K. This advises that the broad transition in the two crystals may have different origins.

The observation that nominal $CePt_3Si$ shows a considerable wide variation of physical properties depending on the heat treatment or on the synthesis procedure may either be indicative of the presence of defects and inhomogeneities and/or of the fact that ternary $CePt_3Si$ does not have a fixed composition in the ternary phase space of Ce-Pt-Si as proposed in Ref. 30. Rather, a solubility range around nominal $CePt_3Si$ would offer a natural explanation for the varying physics observed. Such features are well known for the HFSC $CeCu_2Si_2$ (see, e.g., Ref. 38–40) and have also been observed upon slight changes in stoichiometries in Ce_2Pd_2In.[41] A detailed study of the phase space around $CePt_3Si$ in the ternary phase diagram is in progress.[42]

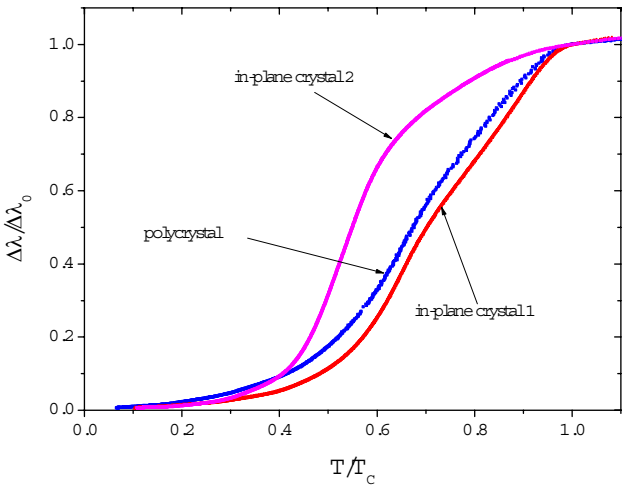

Fig. 2. In-plane penetration depth of single crystals of $CePt_3Si$ from different batches, along with the data of a polycrystalline sample.

3. Normal state properties

Physics in the paramagnetic phase of $CePt_3Si$ and substituted compounds is a result of various competing interactions. The primary ones are the RKKY interaction, the Kondo effect and crystalline electric field (CEF) effects. RKKY interaction is responsible for long range magnetic order in systems with well localised partly filled shells. CEF effects cause a lifting of the $2j + 1 = 6$-fold degenerate ground state associated with the $j = 5/2$ total angular momentum of Ce. The splitting of these states gives rise to strongly modified temperature dependent magnetic properties of the system, creating Schottky anomalies and being also responsible for additional scattering channels in the case of electronic transport. In the following section some of these mechanisms and their mutual interaction will be studied. In order to demerge the various contributions, we will also discuss the substitution of Ce/La, which suppresses both long range magnetic order and superconductivity, leaving over a much simpler paramagnetic state.

Some of the most important features of $CePt_3Si$ and Ce-diluted compounds can be seen from heat capacity data, plotted in Fig. 3 as $\Delta C_p/T$ vs. $\ln T$. $\Delta C_p \sim C_{mag}$ is derived from the data observed experimentally by subtracting the heat capacity of $LaPt_3Si$. At elevated temperatures ($\approx$ 40 K) Schottky anomalies are observed which keep prominent also in the case of the diluted alloys. The center of these anomalies, which does not change significantly upon the Ce/La substitution would imply crystal field levels situated above 100 K. Due to the

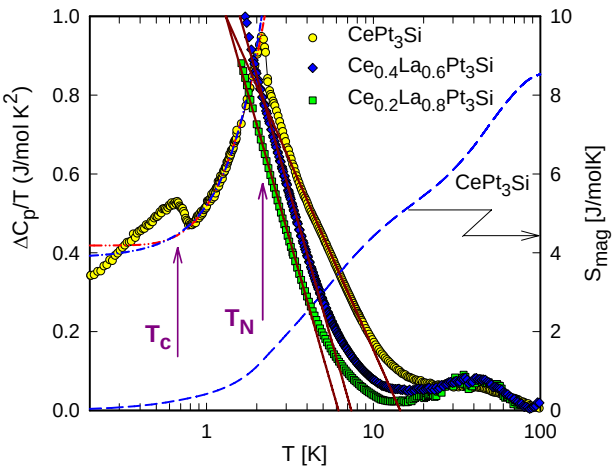

Fig. 3. Temperature dependent magnetic contribution to the specific heat, ΔC_p of $Ce_{1-x}La_xPt_3Si$, $x = 0$, 0.6 and 0.8, plotted as $\Delta C_p/T$ on a logarithmic temperature scale. The phonon contribution to define ΔC_p is taken from $C_p(T)$ of $LaPt_3Si$. The solid straight lines are fits as explained in the text. The dashed-dot-dot and the dashed-dot lines are least squares fits and refer to Eq. 2 and to a T^3 law, respectively. The dashed line represents the magnetic entropy (right axis).

fact that $C_p(T)$ of $LaPt_3Si$ exceeds the measured heat capacity of $CePt_3Si$ at elevated temperatures ($T > 100$ K), an estimation of the spectral weight of this contribution, and thus of details of the CEF level scheme, is not promising. Below about 10 K for $CePt_3Si$ and at lower temperatures for the diluted samples, an almost logarithmic dependence of $\Delta C_p/T$ becomes obvious from Fig. 3, recalling non-Fermi liquid features of systems near to a quantum critical point. According to a phenomenological model developed by Sereni et al.[43] the temperature dependence of the heat capacity of non-Fermi-liquid systems follows from

$$C_p/t = -D \log t + ET_0 \qquad (1)$$

where $t = T/T_0$ and T_0 is a characteristic temperature of the system ($T_0 \sim T_K$, with T_K being the Kondo temperature). The constant D was deduced for most of the non-Fermi-liquids as $D \approx 7$ J/molK and $0 \leq E \leq 0.14$ J/molK^2.[43] Based on this model, T_0 lowers from about 14 K in the case of $CePt_3Si$ to about 6 K for $Ce_{0.2}La_{0.8}Pt_3Si$. This would fit to an increase of the unit cell volume, releasing chemical pressure from the Ce ions. Since the hybridization strength decreases, also the Kondo temperature reduces. The logartihmic feature present at low temperatures even for the most diluted sample, $Ce_{0.2}La_{0.8}Pt_3Si$, evidences that this contribution to the specific heat cannot be associated with short range order effects above a finite temperature magnetic phase transition. Microscopically, this observation may be implicated by a weak feature around 1.4 meV found in our previous inelastic neutron scattering study. The dispersion of the intensity observed at $T = 5$ K, particularly around $Q = 0.8$ Å^{-1} [44] is a signature for the development of short-ranged magnetic correlations and coincides with the anomalous behaviour of the specific heat above magnetic ordering. At higher temperatures ($T \approx 30$ K) scattering becomes Q-independent. This feature is completely absent in non-magnetic $LaPt_3Si$.[44]

A temperature dependence of the heat capacity according to $\Delta C_p/T = \Gamma \log(T_0/T)$ [see the solid line in Fig. 3] would allow to qualitatively account for the logarithmic slope at $T > T_N$, thereby providing the mentioned characteristic temperature $T_0 \sim T_K$. The coefficient Γ would then determine the inital slope in a ΔC_p vs. T plot for $T \to 0$. Here, it should be noted that, while $\Delta C_p/T = \Gamma \log(T_0/T)$ diverges for $T \to 0$, $\Delta C_p = T\Gamma \log(T_0/T)$ tends towards 0. A least squares fit to the present data reveals $T_0 = 14.5$, 7.8, and 6.1 K, while $\Gamma = 0.9$, 1.39 and 1.48 J/molK^2, for the compounds $x = 0$, 0.6 and 0.8, respectively. An intrinsic feature of that logarithmic temperature dependence would be a local maximum in a ΔC_p vs. T plot, roughly around $T_0/3$. In fact, the present data show smooth maxima at 5, 2.8 and 2.1 K, for $x = 0$, 0.6 and 0.8, respectively. The height of that local maximum, $\Delta C_p^{max} = 0.16\Gamma T_0$, is affected from a balance of both Γ and T_0. Also, Takeuchi et al.[29] have recently noticed such a local maximum around 5 K in $CePt_3Si$, but not definite explanation was given about the nature of that anomaly.

Concerning the ordered phase, long range magnetic order sets in at $T_N = 2.25$ K, evidenced from the pronounced anomaly in $\Delta C_p/T$. The AFM character of this phase is confirmed by a slight shift of this anomaly towards lower temperatures along with increasing external magnetic fields. To quantitatively account for the thermal properties of that region, a model proposed by Continentino et al.[45] is applied well below T_{mag}:

$$C_{mag} = g\Delta^{7/2}T^{1/2}\exp(-\Delta/T) \times \left[1 + \frac{39}{20}\left(\frac{T}{\Delta}\right) + \frac{51}{32}\left(\frac{T}{\Delta}\right)^2\right], \qquad (2)$$

Eqn. 2 is based on antiferromagnetic magnons with a dispersion relation given by $\omega = \sqrt{\Delta^2 + D^2k^2}$, where Δ is the spin-wave gap and D is the spin-wave velocity; $g \propto 1/D^3 \propto 1/\Gamma^3$ and Γ is an effective magnetic coupling between Ce ions. A least squares fit of Eq. 2 to the data below T_N (solid line, Fig. 3) reveals $\Delta \approx 2.7$ K, a reasonable gap value with respect to the ordering temperature. Another model calculation with simple antiferromagnetic spin waves with $C_{mag}^{AFM} \propto T^3$ gives reasonable agreement with the data, too. Using both models, we estimate a Sommerfeld coefficient of 0.41 and 0.39 J/molK^2 for the former and latter models, respectively. These figures are also in good agreement with an extrapolation of high field specific heat data where SC is suppressed by applying magnetic fields.[23] A recent neutron diffraction study on $CePt_3Si$ reveals antiferromagnetic ordering below $T_N \approx 2.2$ K with a wave vector $\vec{k} = (0, 0, 1/2)$, i.e. doubling of the magnetic unit cell along $\vec{c}$-direction.[46]

Previously performed specific heat measurements on single crystalline $CePt_3Si$ revealed $T_N = 2.25$ K at the very same temperature, but the anomaly appears to be sharper and the specific heat jump right at T_N is larger by about 10 %.[29] A fit to that data-set confirms a T^3 dependence and yields $\gamma_n = 0.335$ J/molK^2, a value slightly below the above indicated ones.

The temperature dependent magnetic entropy, S_{mag}, is plotted as dashed line and refers to the right axis of Fig. 3. Although there are difficulties to evaluate $\Delta C_p(T)$ and thus $S_{mag}(T)$ at high temperatures ($T > 100$ K), the data below the 50 to 100 K range are credibly. The integrated entropy up to 20 K is nearly $R \ln 2$, (=5.76 J/molK) and the entropy of 8.7 J/molK integrated up to 100 K is less than $R \ln 4 = 11.5$ J/molK. These results evidence that the ground state of the Ce^{3+} ions is a doublet, while the the first excited CEF level lies above 100 K. The release of magnetic entropy in the low temperature range up to about 20 K makes it rather unlikely that CEF effects cause levels which are almost degenerate, or where the splitting is very small, of the order of 1 or 2 meV. This is in line with the general observation that quartets or quasi-quartets are rarely found in Ce-site symmetries lower than cubic.

Also, the magnetic entropy release at $S_{mag}(T = T_N) \approx 0.2R \ln 2$ is well below that figure expected for magnetic ordering of localised magnetic moments in a CEF doublet as ground state. This missing entropy at $T = T_N$ is usually interpreted in terms of a Kondo screening of magnetic moments. Furthermore, the large Sommerfeld value γ refers to Kondo interaction, forming heavy quasi-particles. Taking into account only magnetic entropy data allows to estimate the Kondo temperature $T_K \approx 7.2$ K from numerical results derived in Ref. 47. A second possible estimate of T_K stems from the competition of the RKKY interaction and the Kondo effect, which leads to a significant reduction of the specific heat jump at $T = T_N$. Following the procedure developed in Ref. 48 gives $T_K \approx 9$ K, in reasonable agreement with the previous estimate. A characteristic temperature of the order of 10 K was derived from the non-Fermi liquid features of the specific heat as discussed above.

Measurements of electronic transport are considered as indispensable tools for discussing Kondo type interaction and CEF effects.[49] Results of temperature dependent resistivity measurements on a series of compounds where Ce is substituted by La in $CePt_3Si$ are plotted in Fig. 4(a). Data are normalised to room temperature in order to pronounce a number of distinct features. Starting with nonmagnetic $LaPt_3Si$ one reveals information concerning the electron - phonon interaction in terms of the simplified Debye model. Within this scenario, the resistivity can be accounted for by the Bloch-Grüneisen law yielding a temperature independent electron - phonon interaction constant and the Debye temperature θ_D. The latter follows from a least squares fit as $\theta_D \approx 160$ K.[23] Exchanging La by Ce in $LaPt_3Si$ causes a gradual change of the resistivity features in the paramagnetic temperature range: i) for temperatures from about 50 to 100 K, a pronounced shoulder develops as a consequence of CEF splitting of the Ce $j = 5/2$ total angular momentum. ii) at low temperatures, a distinct minimum arise, a key feature of Kondo type interaction in diluted magnetic systems.

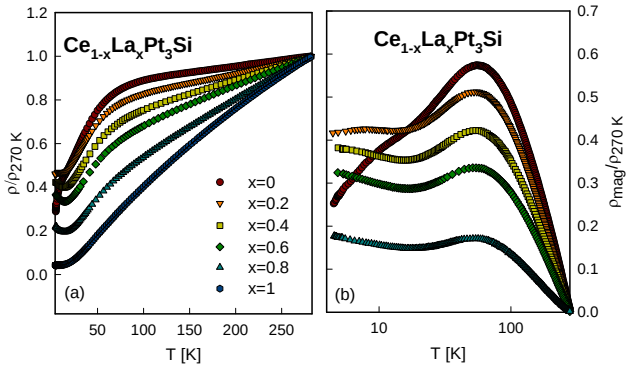

Fig. 4. (a) Normalized electrical resistivity, $\rho/\rho_{270\ \mathrm{K}}$, of $(Ce, La)Pt_3Si$. (b) Temperature dependent magnetic contribution to the electrical resistivity, ρ_{mag}, of $(Ce, La)Pt_3Si$

In order to better resolve the various characteristics of $\rho(T)$, we have subtracted the non-magnetic background as defined by $LaPt_3Si$. This procedure was carried out using absolute $\rho(T)$ values of the different samples. Results are shown in Fig. 4(b) as ρ_{mag} vs. $\ln T$, again in a normalized representation. The logarithmic contributions to the electrical resistivity at low and at high temperatures, separated by a maximum, refer to a textbook-like example of the Kondo effect in presence of strong CEF splitting.[49] The latter is responsible for a lifting of the 6-fold degenerate ground state into 3 doublets. This follows by very general arguments from a $j = 5/2$ total angular momentum in the context of a tetragonal crystal structure. The figure allows the following propositions: i) The overall crystal field splitting is essentially unchanged by the Ce/La substitution (i.e., T_ρ^{max} in $\rho_{mag}(T)$ remains constant). Due to the lattice expansion upon the Ce/La substitution, one would expect a change of the Coulomb interaction, resulting in some modification of the CEF level scheme. ii) The negative logarithmic contributions at low temperatures refer to the Kondo effect in the CEF ground state. This behaviour makes the existence of a low lying (10 to 20 K) CEF doublet rather unlikely. The latter was proposed by Metoki et al.[46] from inelastic neutron scattering (INS) experiments, but both specific heat as discussed above and another set of INS data[50] seem to be corroborated by the electronic transport data. In fact, previously performed INS experiments at the HMI Berlin with high resolution at low incident neutron energies carried out at low temperatures failed to resolve any inelastic excitation of magnetic origin.[51] A low lying doublet above the ground state seems to be rather unlikely and thus the physics at the lowest temperatures is primarily defined from the ground state doublet only.

The effect of an external magnetic field on the electrical resistivity is shown for the series of $(Ce, La)Pt_3Si$ at $T = 2$ K in Fig. 5 . The change of the electrical resistivity upon the application of an external magnetic field can roughly be divided into two parts. The first, so called *classical magnetoresistance*, is due to the Lorenz force, acting on the electrons which are moving in response to an electrical field gradient. This classical contribution is present in each metallic material. The second arises from the magnetic field dependence of the quantum mechanical scattering processes and is usually known as

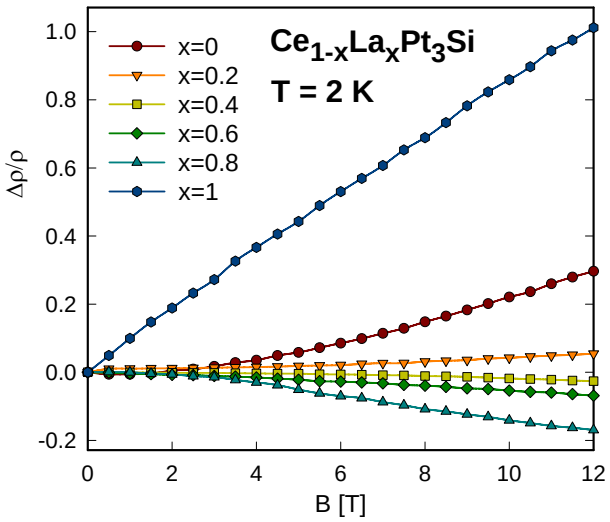

Fig. 5. Isothermal magnetoresistance $\Delta\rho/\rho$, for various compounds of (Ce, La)Pt_3Si at $T = 2$ K.

non-classical magnetoresistance. It contributes to the resistivity whenever magnetic scattering processes have to be taken into account.

The present sample series provides a possibility to determine how the classical magnetoresistance is modified by the non-classical one by the increament of the Ce content. Starting with nonmagnetic $LaPt_3Si$ one observes an almost linear increase of $\Delta\rho/\rho$ as a function of the applied magnetic field. At $B = 12$ T, $\Delta\rho/\rho$ reaches values of the order of 100 %. In classical, single band systems, the magnetoresitance in the low field limit, i.e., $\omega\tau < 1$ where ω is the cyclotron frequency and τ is the relaxation time, is expected to follow a quadratic dependence in B, i.e.,

$$\rho(T, B) = \rho(T) + a^2(T)B^2 \quad , \tag{3}$$

This is a very obvious result since in view of Onsager's relation one expects only even powers in B within a series expansion of $\rho(B)$. Obviously, $LaPt_3Si$ does not follow such a quadratic law which, most likely, is a consequence of the multiband structure of $LaPt_3Si$. Missing of inversion symmetry triggers a strong spin-orbit coupling thereby splitting the Fermi surface into subbands.

Ce embedded in $LaPt_3Si$ dramatically changes the isothermal magnetoresistance; instead of an increase of the resistivity as a function of field, a decrease is observed when the field strength rises. Such an observation is a clear hint to magnetic scattering processes, which become important upon the presence of almost trivalent magnetic Ce^{3+} ions. Moreover, it is obvious that the increase of the Ce content - roughly within the single impurity range - causes an enlargement of the absolute magnitude of $\Delta\rho/\rho$. In terms of a model by Schlottmann,[52] developed for Kondo systems with $j = 1/2 \ldots 7/2$, the magnetoresistance $\rho(B)/\rho(0)$ is a universal function of (B/B^*), showing that the physics of Kondo systems is determined by a single characteristic energy scale, $\mu_B B^* \sim k_B T_K$. As this temperature scale grows for a certain series, the Kondo related magnetoresistance becomes smaller at a given external magnetic field. Since there is no reliable method available to separate the non-classical contribution from the classical one, fits are meaningful only if the non-classical contribution dominates the classical one. Nevertheless, the conclusion which may be drawn here is that the increase of the Ce content also increases the characteristic Kondo temperature T_K. Physically, this follows from the reduction of the unit cell volume if the larger La ions are exchanged by smaller Ce, stressed already in conjunction with the specific heat data. Finally, if $CePt_3Si$ is approached, the magnetoresistance becomes positive again. It is well known from literature that Kondo lattices may exhibit positive magnetoresistances at low temperatures, which theoretically is corroborated from calculations performed in terms of the periodic Anderson lattice model.[53]

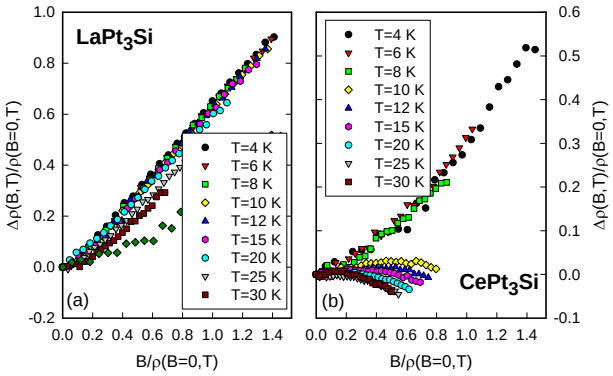

Fig. 6. Kohler plot of (a) $LaPt_3Si$ and (b) $CePt_3Si$.

In order to show that there are distinct differences in the case of the positive magnetoresistance of both $LaPt_3Si$ and $CePt_3Si$, the Kohler rule, i.e.,

$$\frac{\rho(B,T) - \rho(B=0,T)}{\rho(B=0,T)} = f\left(\frac{B}{\rho(B=0,T)}\right) \tag{4}$$

is applied. According to Eq. 4, the magnetoresistance of a metal is a well behaving function f of $B/\rho(B = 0)$. Rigorously, Eq. 4 can be justified only in a single-band model. Fortunately Kohler's rule has been found as a good approximation in many cases where *one* scattering mechanism dominates. Since electron-phonon interaction in $LaPt_3Si$ is the dominant scattering term, it is expected that a Kohler plot will condense all the isothermal data from the various temperatures onto a single curve, while equally important electron-phonon and electron-magnetic moment scattering do no longer satisfy the requirements of Kohler's model. Results of such an analysis are represented in Fig. 6.

Obviously, the magnetoresistance of $LaPt_3Si$ for the various temperatures observed matches a single function f while that of $CePt_3Si$ clearly fails. This indicates that the positive magnetoresistance derived for the latter is of different origin in comparison to the one found for $LaPt_3Si$.

The temperature and field dependent resistivity of $CePt_3Si$ is displayed in Fig. 7(a). The sample investigated here exhibits a larger residual resistivity, $\rho_0 \approx 11$ $\mu\Omega$cm, than the one studied previously in Ref.

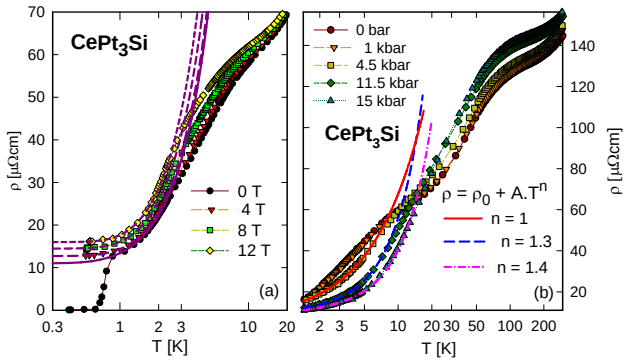

Fig. 7. (a) Temperature dependent electrical resistivity of $CePt_3Si$ at various magnetic fields. The lines are least squares fits explained in the text. (b) Temperature dependent electrical resistivity of $CePt_3Si$ at various pressures. The lines are least squares fits explained in the text.

23. Nevertheless, superconductivity occurs at about the same temperature, $T_c \approx 0.75$ K, indicating that disorder scattering does not play a crucial role. The application of magnetic fields causes an increase of the overall $\rho(T)$ values, as already concluded from isothermal results of Fig. 5.

In order to qualitatively account for the ordered region of $CePt_3Si$, the model developed for heat capacity data below T_N can also be adopted for resistivity:[45]

$$\rho(T) = \rho_0 + C\Delta^{3/2}T^{1/2} \times \quad (5)$$
$$\times \exp(-\Delta/T)\left[1 + \frac{2}{3}\left(\frac{T}{\Delta}\right) + \frac{2}{15}\left(\frac{T}{\Delta}\right)^2\right],$$

where ρ_0 is the residual resistivity and C is a material dependent constant. Results of least squares fits are shown as lines in Fig. 7(a). The principal finding is that Δ grows from 1.8 K at zero field to 3 K at 12 T.

The pressure response of $\rho(T)$ of $CePt_3Si$ is plotted in Fig. 7(b) for temperatures above 1.5 K. As the externally applied pressure increases, the absolute values of $\rho(T)$ start to increase at high temperatures, but decrease at low temperatures. The residual resistivity in such kind of compounds constitutes from the usual lattice imperfections which do not alter the Kondo lattice and various types of imperfections which influences the Kondo resonance and act like a Kondo hole, similar to magnetic impurities in a non-magnetic host.[54] Graf et al.[55] have demonstrated that $\rho_0 \propto m^* \sin^2 \eta$, with η being the phase shift in scattering processes. Since T_K of Ce systems is enhanced by pressure, m^* decreases, basically originating the lowering of $\rho_0(p)$, too.

Pressure also causes a significant change of the low temperature resistivity. It has been demonstrated[56,57] that increasing pressure suppresses both, long range magnetic order ($p_{c1} \approx 6-8$ kbar) and superconductivity ($p_{c2} \approx 15$ kbar). The vanishing of antiferromagnetic order in $CePt_3Si$ at medium pressure ranges allows to trace the crossover from long range magnetic order towards a paramagnetic state, thereby passing, most likely, a quantum critical point. In fact, least squares fits according to $\rho = \rho_0 + AT^n$ show that $\rho(p,T)$ renders this evolution: A linear behaviour in $\rho(T)$ is obtained for $p_1 = 4.5$ kbar, with $p_1 \approx p_{c_1}$. Besides the negative logarithmic contribution to the specific heat, $\rho(T) \propto T$ is another signature of non-Fermi liquid physics. The increase of pressure gradually suppresses spin fluctuations, allowing to establish a Fermi liquid ground state with $n = 2$ which, however, is not achieved within the pressure range presently used.

The high temperature resistivity shoulder, corresponding to the the overall CEF splitting Δ_{CEF}, linearly decreases from about 58 K to 55 K when changing the pressure from 1 bar to 15 kbar, respectively. This result is unexpected, since in terms of a point charge model, approaching of ions enhances Coulomb interaction. Thus, an enlargement of CEF level energies is expected. Details of the DOS near E_F may be a possible cause of this unattended observation.

The pressure and field dependence of a diluted system, $Ce_{0.4}La_{0.6}Pt_3Si$, is highlighted in Fig. 8(a),(b). Different to the parent compound, the residual resistivity obviously increases with increasing pressure. According to the scenario sketched above, the phase shift η may overcome the decrease of the m^* possibly due to the largely grown statistical disorder in the substituted compound. It is interesting to note that this dilute system shows pronounced hints of coherence, evidenced from the low temperature maximum in $\rho(T)$ around 2.5 K and the subsequent decrease when further decreasing the temperature. Also different with respect to $CePt_3Si$, the application of magnetic fields diminishes $\rho(T)$. In accordance to the temperature dependence of this sample, Kondo type scattering, which becomes quenched in high magnetic fields, is accountable for. The magnetoresistance at 2 K and 12 T is about -15 %. Another convincing arguement that there is no low lying CEF level comes from the observation that the low temperature maximum in $\rho(T)$ of $Ce_{0.4}La_{0.6}Pt_3Si$ shifts substantially to higher temperatures when the field strength increases. This dependence marks somehow a formal increase of the Kondo temperature T_K with growing fields. If the same structure in $\rho(T)$ would correspond to a CEF effect, magnetic fields could hardly originate such a distinct shift. Rather, they would cause an broadening of the structure due to a Zeeman splitting of the levels.

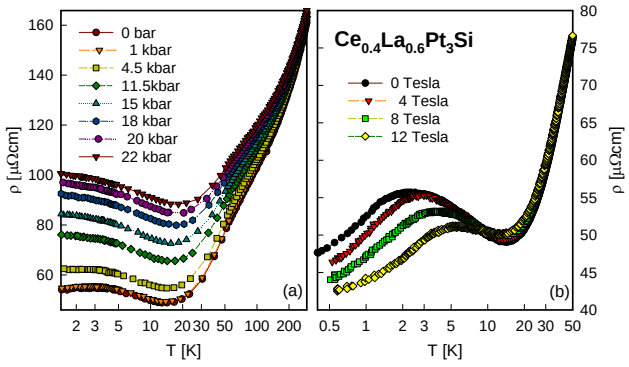

Fig. 8. Temperature dependent electrical resistivity, ρ, of $Ce_{0.4}La_{0.6}Pt_3Si$ at (a): various values of applied pressure and (b): magnetic fields.

4. Superconducting Properties of $CePt_3Si$

Similar to the physics in the normal state region, specific heat data are helpful for understanding complex mechanisms present in the superconducting ground state. A careful analysis of the heat capacity taken on a polycrystalline sample is shown in Fig. 9. In order to avoid phononic and antiferromagnetic contributions, a T^3 term (dashed line) is subtracted from the raw data; results are shown in Fig. 9 as dark squares in a C_p/T vs. T representation. This analysis provides the normal state Sommerfeld value $\gamma_n \approx 390$ mJ/molK^2 in an intuitive manner, satisfying the entropy balance between the normal and the superconducting state.

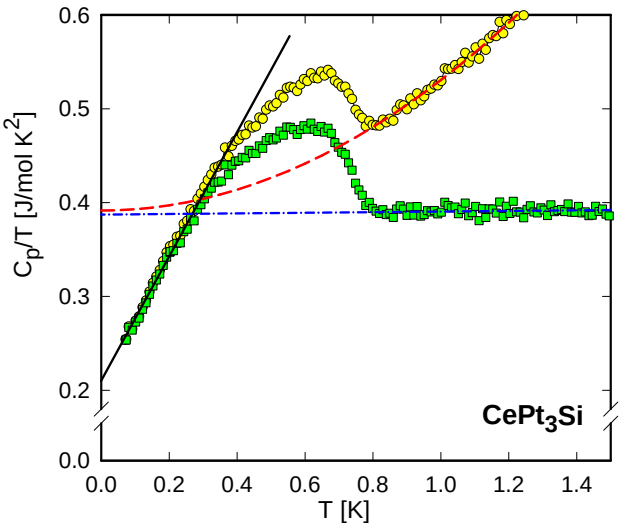

Fig. 9. Temperature dependent specific heat C_p/T of $CePt_3Si$ (light spheres); the dashed line is a T^3 extrapolation of $C_p(T)$. The dark squares are the heat capacity data reduced by the antiferromagnetic contribution. The dashed-dot line is a linear extrapolation towards zero. The solid line illustrates a T^2 behaviour of the specific heat at very low temperatures.

At lower temperatures, the heat capacity, corresponding to the quasiparticle density of states, exhibits a T^2 behaviour rather than an exponential dependence (solid line, Fig. 9). This would refer to a gap structure with line-nodes. Assuming line nodes in the $x-y$-plane, i.e, $\Delta_{\vec{k}} = \Delta_m \cos\theta$ (Δ_m is the maximum gap width), one obtains the density of states $N(E)$ as[1]

$$N(E) = N_0 \frac{E}{\Delta_m} \begin{cases} \frac{\pi}{2} & |E| < \Delta_m \\ \arcsin\left(\frac{\Delta_m}{E}\right) & |E| \geq \Delta_m \,. \end{cases} \quad (6)$$

Eq. 6 evidences a finite density of states below the maximal gap and down to zero energy. $N(E)$ vanishes linearly for $E \to 0$ and the singularity at $E = \Delta_m$ in fully gapped systems is replaced by a cusp. As a result, the anisotropy smooths singularities derived in the isotropic gap case. Using standard thermodynamics, the specific heat can be expressed as

$$C(T) = \int dE N(E) \frac{E^2}{k_B T^2} \frac{1}{4\cosh^2(E/2k_BT)} \quad (7)$$

Simple scaling in the integral shows that a power law in the density of states, i.e., $N(E) \propto E^n$ for $E \to 0$ translates directly to a power law in the temperature dependence:[1]

$$C(T) = \int dE E^n \frac{E^2}{k_B T^2} \frac{1}{4\cosh^2(E/2k_B)} \propto T^{n+1}. \quad (8)$$

Employing $N(E)$ of Eq. 6 yields a T^2 dependence of the heat capacity at low temperatures instead of an exponential behaviour for the case of an isotropic gap. This particular result favours the assumption of line-nodes being present in $CePt_3Si$. A similar conclusion was drawn from the heat capacity study performed on single crystalline material.[29]

Extrapolating the linear dependence of $C_p/T(T)$ towards zero reveals a residual electronic specific heat coefficient in the superconducting state of $\gamma_s \approx 200$ mJ/molK^2. A smaller value of 34 mJ/molK^2 was found in the single crystal study of Takeuchi et al.[29] The finite γ_s value may be a consequence of the gapless superconducting state presumably due to line-nodes of the order parameter and/or may follow from normal state sheets of the Fermi surface which might be responsible as well for long range magnetic order below 2.25 K. Additionally, the jump of the specific heat anomaly associated with superconductivity, $\Delta C_p/T|_{T_c} \approx 0.1$J/molK^2, leads to $\Delta C_p/(\gamma_n T_c) \approx 0.25$, which is significantly smaller than the figure expected from the BCS theory, $\Delta C_p/(\gamma T_c) \approx 1.43$. This diminished jump at $T = T_c$ is not a result of an inferior sample quality associated with the polycrystalline material, since also the single crystal measurement on $CePt_3Si$[29] revealed $\Delta C_p/(\gamma_n T_c)$ well below the BCS value. Thoroughly studied spin triplet superconductor Sr_2RuO_4 shows similar figures.[58]

Evidence for coexistence of superconductivity and long range magnetic order has recently been obtained from μSR measurements.[59] In real space, both states appear to be *not* spatially segregated. A competition of both phenomena seems to be absent, i.e., the share of electrons responsible for long range magnetic order does not change if the system enters the superconducting state. These μSR studies also demonstrated the bulk character of the antiferromagnetic state below T_N. Such conclusion was based on the amplitude of the magnetic μSR signal, formed by two components corresponding to two distinct muon sites. As one of them is characterised by an internal field $B_\mu \simeq 0$, we recently performed additional transverse-field μSR studies by concentrating our investigations on muons stopping at this site. In a field-cooling procedure, the depolarization rate of this component, measured in a external field of 500 G, did not show any change when crossing the superconducting transition (see Fig. 10). As an increase of the field distribution is expected due to the presence of a flux line lattice, such absence of anomaly at T_c could be indicative either of the absence of bulk superconductivity or of a rather large value of the London penetration depth. To differentiate between these scenarii, zero-field cooling experiments were performed, which clearly indicate an increased field distribution in the superconducting state.

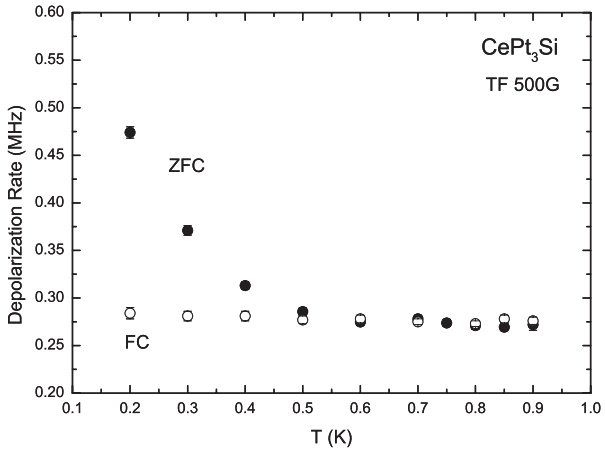

Fig. 10. Temperature dependence of the μSR depolarization rate obtained in an external transverse field of 500 G. The reported data refer solely to the component of the μSR signal with weak internal field arising from the AFM state (see test and Ref.[59] for details). Note the drastic difference between field-cooling and zero-field-cooling procedure.

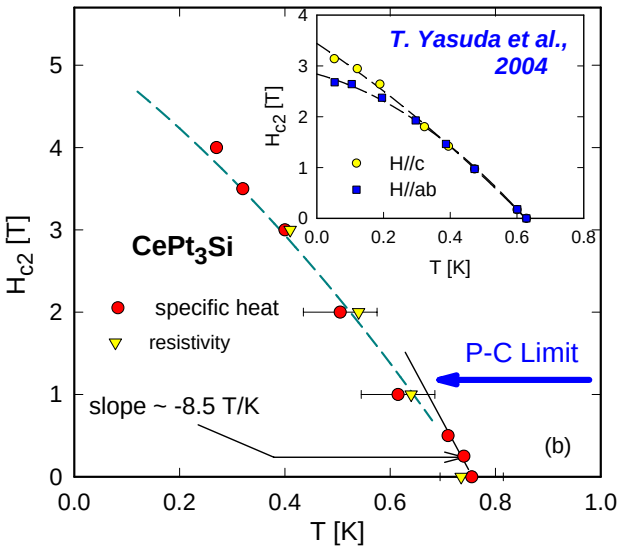

Fig. 11. Temperature dependence of the upper critical field H_{c2}. The solid straight line yields $H'_{c2} \approx -8.5$T/K; the dashed line is a guide to the eyes (Ref.[23]). PC indicates the Pauli - Clogston limiting field. The inset shows measurements of H_{c2} on a single crystalline $CePt_3Si$ sample with fields along and perpendicular to the $\vec{c}$ axis. Data are taken from Ref.[60]

Such ZFC measurements therefore rule out the scenario of non-bulk superconductivity and implicitly confirm the microscopic coexistence between AFM and SC states. In addition the absence of any anomaly in the FC procedure sets a lower limit for the value of the penetration depth of 900 nm. Such limit is compatible with a previous thermodynamic determination of the penetration depth, compare Table 1.

What triggered most of the theoretical efforts to understand superconductivity in absence of inversion symmetry was the observation that the upper critical field $H_{c2}(0) \approx 4$ T exceeds the Pauli-Clogston limit $H_p \approx 1.1$ T by far, implying that the Zeeman splitting must be non-negligible below T_c. The temperature dependence of H_{c2} is shown in Fig. 11. The same order of magnitude for the upper critical field was derived from measurements on a single crystal[60] (compare inset, Fig. 11). The absence of Pauli limiting, in a first view, would be indicative of spin triplet pairing. A theorem by Anderson,[10] however, points out that inversion symmetry is a key element for spin-triplet paired states to occur. Missing the mirror plane along the $\vec{c}$-axis should thus be harmful for a spin-triplet scenario in $CePt_3Si$.

Absence of inversion symmetry in a crystal lattice gives rise to internal fields that affects in a very general manner electronic properties by antisymmetric spin-orbit coupling. Similarly to Zeeman coupling, it causes a splitting of electronic bands, thereby removing the spin degeneracy. The strength of the splitting is measured by a constant α, which in the case of $CePt_3Si$ was estimated to be of the order of 1000 K.[61] Each of the Fermi surfaces thus consists of two kinds of areas, similar in topology but slightly different in volume. Experimentally, this splitting was already found from deHaas van Alphen studies for $LaPt_3Si$, isostructural to $CePt_3Si$.[62]

Based on the framework of a Rashba-like splitting of the Fermi surface, Frigeri et al.[63] promoted a model where they could show that the antisymmetric spin-orbit coupling is not destructive to spin triplet pairing in any case. Rather, some special spin-triplet states with $\vec{d}(\vec{k}) \parallel \vec{g}_{\vec{k}}$ appear to be unaffected by the absence of inversion. Here, $\vec{d}(\vec{k})$ refers to the spin-triplet part of the gap function $\Delta(\vec{k})$ and the antisymmetric vector $\alpha\vec{g}_{\vec{k}}$ characterises and quantifies the absence of an inversion centre in the crystal. $\vec{g}_{\vec{k}}$ can be determined by symmetry arguments and is normalized as $\langle \vec{g}^2_{\vec{k}} \rangle_0 = 1$. The brackets denote the average over the Fermi surface in the case of $\alpha = 0$. For $\alpha\vec{g}_{\vec{k}} = 0$, the split Fermi surfaces touch each other again. Based on group theoretical arguments concerning the space group $P4mm$ of $CePt_3Si$, which has C_{4v} as the generating point group, with the reflection symmetry being absent for $z \to -z$, $\vec{g}_{\vec{k}}$ corresponds to $\vec{g}_{\vec{k}} = (k_y, -k_x, 0)/k_F$, where k_F is the Fermi wave vector of a simplified spherical Fermi surface. A characteristics of $\vec{g}_{\vec{k}}$ is that it vanishes along the $\vec{z}$-axis for $k_x = k_y = 0$. The most stable pairing state for $\vec{d}(\vec{k}) \parallel \vec{g}_{\vec{k}}$ appears to be of p-type $\vec{d}(\vec{k}) = \hat{x}k_y - \hat{y}k_x$, while the Balian Werthamer state without nodes, $\vec{d}(\vec{k}) = \hat{x}k_x + \hat{y}k_y + \hat{z}k_z$, would have signficantly reduced transitions temperatures.[63]

Frigeri et al.[63] have also shown that paramagnetic limiting is absent for all $\vec{k}$, $\vec{H} \perp \vec{d}(\vec{k})$ and $\vec{d}(\vec{k}) \parallel \vec{g}_{\vec{k}}$. The protected spin-triplet state $\vec{d}(\vec{k}) = \hat{x}k_y - \hat{y}k_x$, i.e., $\vec{d}(\vec{k}) = \vec{g}_{\vec{k}}$, would thus provide an explanation for the absence of paramagnetic limiting in $CePt_3Si$. Even in the case of spin-singlet pairing, paramagnetic limiting becomes less effective in the presence of spin-orbit coupling, and the paramagnetic limiting field continuously grows with growing α.[63] Furthermore, the suppression of paramagnetism is expected to be very anisotropic for fields along the $\vec{c}$-axis and within basal plane.[11,64]

The inset of Fig. 11 shows single crystal measure-

ments,[60] revealing slightly smaller values of the upper critical field in comparison to the polycrystalline material. The striking feature, however, is that the anisotropy deduced from measurements parallel and perpendicular to the $\vec{c}$-axis is rather small, i.e., $H_{c2}^{c}/H_{c2}^{ab} \approx 1.18$ for $T \to 0$. For fields along the $\vec{c}$-axis, paramagnetic limiting is absent because $\vec{g}_{\vec{k}}\vec{H} = 0$; $[\vec{g}_{\vec{k}} = (k_y, -k_x, 0)/k_F]$. The vortex phase is expected to be quite conventional.

In order to get rid of the distinct reduction of the in-plane paramagnetic effect in $CePt_3Si$, a helical structure of the order parameter was proposed by Kaur et al.[65] In the case of $\vec{H} \perp \vec{c}$, the field can induce a phase which gives rise to an additional phase factor $\exp(i\vec{q}\vec{R})$ in the many body wave function; $\vec{q}$ is perpendicular to the applied field. This creates a helical vortex phase, expected to explain the diminishing of paramagnetic limiting. The enhancement of H_{c2} due to such a helical order can be substantial.[65] Here, it should be noted that the phenomenological origin of the helical phase and that of a FFLO phase singlet superconductor with a spatially oscillating order parameter is very different.[66] In a microscopic picture the origin of the helical phase is the magnetic field induced shift of the center of the Fermi seas away from $\vec{k} = 0$.[65]

An important feature of the spin-triplet state $\vec{d}(\vec{k}) = \hat{x}k_y - \hat{y}k_x$ is the absence of nodes. As pointed out above, the specific heat measurements suggest the existence of line nodes in the gap structure. A powerful tool for probing the presence or not of nodes in the gap is the temperature dependence of the magnetic penetration depth $\lambda(T)$. This quantity is entirely connected with the superfluid density, thus it is *not* related with other preponderant interaction processes, such as the long range magnetic order already acquired for $CePt_3Si$. The London penetration depth is thus a very feasible tool to study the low-energy excitation spectrum of the quasiparticles associated with the superconducting gap topology. Fig. 12 shows results, obtained using a tunnel diode oscillator system running at 9.5 MHz, for polycrystalline and single crystal samples of $CePt_3Si$ in the temperature region from T_c down to 0.050 K.[28,67] Fig. 12(a) depicts the normalized variation of $\Delta\lambda(T)/\Delta\lambda_0$ versus T/T_c in the whole temperature region. Here $\Delta\lambda(T) = \lambda(T) - \lambda(0.050K)$ and $\Delta\lambda_0$ is the total penetration depth shift. There are several intriguing features in these data, in particular the broad transition (obvious also from resistivity measurements[23]) and the inflection point around 0.52 K. They both could be related to the second superconducting transition implied by the specific heat data, as discussed above. Fig. 12(b) displays $\Delta\lambda(T)$ vs T/T_c in the low temperature range $T < 0.2T_c$. It can be clearly seen that the penetration depth data of both type of samples (single crystal and polycrystal) follow a linear temperature behaviour below $0.17T_c$.

For a clean, local superconductor the penetration depth is given by

$$\frac{\lambda^2(0)}{\lambda^2(T)} = \left[1 + 2\left\langle \int_{\Delta}^{\infty} dE \frac{\partial f}{\partial E} \frac{E}{\sqrt{E^2 - \Delta^2(T,\theta,\phi)}} \right\rangle\right]. \quad (9)$$

Here $\langle \cdots \rangle$ represents an angular average over the Fermi surface and f is the Fermi function. Evidently the temperature dependence of $\lambda(T)$ depends on the topology of the gap structure. For line nodes in the energy gap the penetration depth is expected to be linear in the low temperature limit, where the temperature dependence of the energy gap can be neglected. Assuming that $CePt_3Si$ is both a clean ($l > \xi_0$) and a local ($\lambda(0) > \xi_0$) superconductor (compare Table 1), the penetration depth experimental results point out to the existence of lines of nodes in the structure of the superconducting pairing state and, hence, to unconventional superconductivity in $CePt_3Si$.

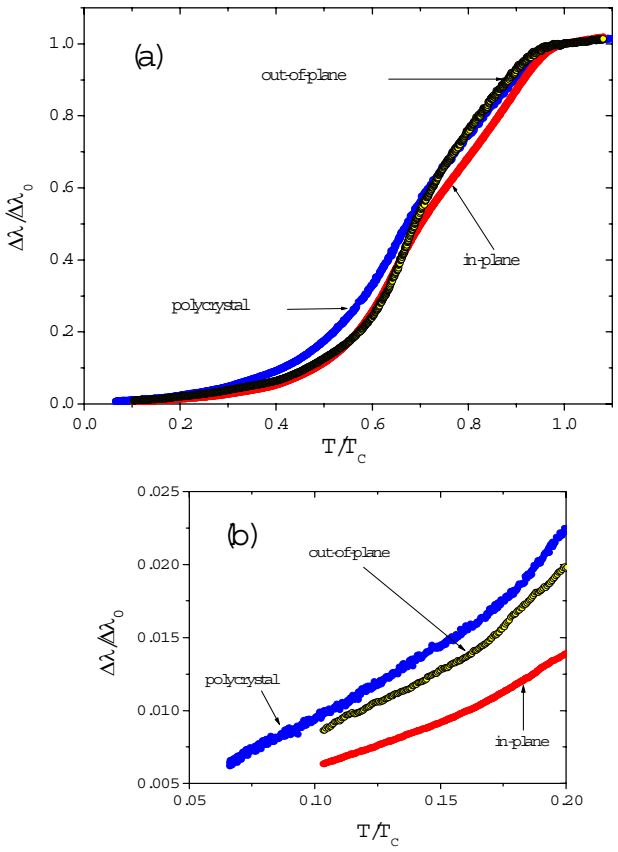

Fig. 12. (a) Normalized variation $\Delta\lambda(T)/\Delta\lambda_0$ versus T/T_c in $CePt_3Si$ samples. (b) Low temperature region in $\Delta\lambda(T)$ displaying a linear temperature behavior.

Figure 13(a) shows the normalized superfluid densities against T/T_c for a single crystal of $CePt_3Si$.[67] The strong suppression of the responses at high temperatures is similar to the one found in polycrystals.[28] The more rapid increase in the response of $\rho(T)$ below about $0.67T_c$ (displayed as a second drop in the penetration depth) is more pronounce in single crystal than in polycrystals data. Fig. 13(b) displays the anisotropy of the superfluid density of $CePt_3Si$ determined from the data of Fig. 13(a). The anisotropy exhibits a nonmonotonic behavior, and because of the upturn observed at high temperatures such a behavior is realized in a more complex form than that predicted by the model of Hayashi *et al.*[68]

Another microscopic information about the superconducting state present in $CePt_3Si$ can be obtained from the temperature dependent nuclear spin-relaxation rate

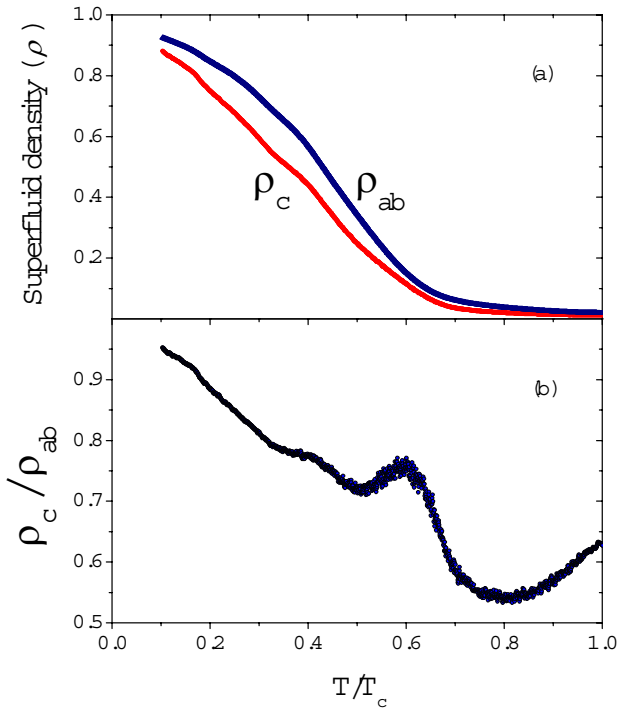

Fig. 13. (a) In-plane (ρ_{ab}) and out-of-plane (ρ_c) components of $\rho(T)$ against T/T_c for a single crystal of $CePt_3Si$. (b) Temperature dependence of the anisotropy of the superfluid density.

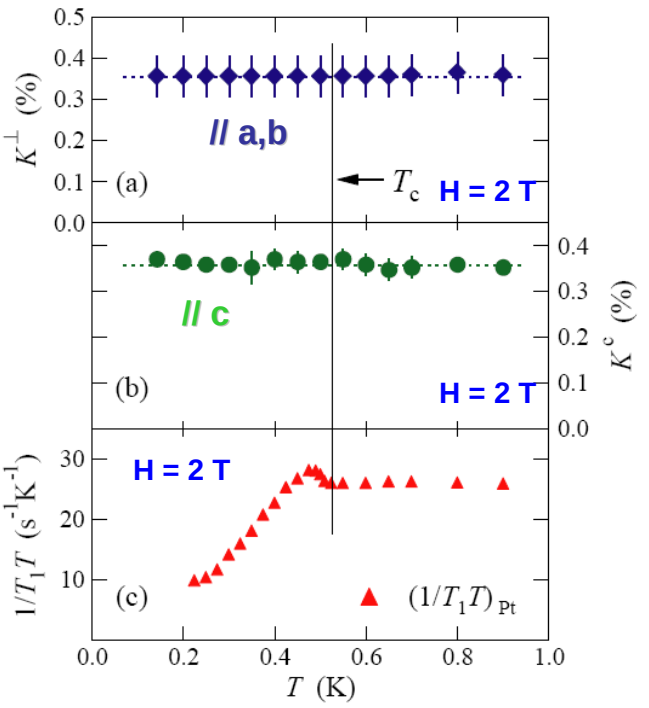

Fig. 14. Temperature dependent Knight shift $K^{\perp}$ ($H \perp \vec{c}$-axis). (a) and $K^{\parallel}$ ($H \parallel \vec{c}$-axis) (b) of $CePt_3Si$ at $H = 2$ T. (c): $1/T_1$ NMR relaxation rate of $CePt_3Si$ at $H = 2$ T. Data taken from Ref. 70.

$1/T_1$ and from the NMR Knight shift.[69,70] Results are shown in Fig. 14. The most exceptional feature in the temperature dependence of the $1/T_1$ relaxation rate [Fig. 14(c)] of $CePt_3Si$ is a kind of Hebel-Slichter anomaly right at T_c,[71] indicating coherence effects as in conventional BCS SC. Neither an exponential law as in BCS superconductors nor the usual T^3 dependence, reported for most of the unconventional HF SC (see e.g., Ref. 72 and Refs. therein), is able to account for the data in the entire temperature range.[69] Rather, data seem to start following the line-node model at the lowest measured temperatures, while for $T \approx T_c$, the temperature dependence of $1/T_1$ is reasonably well described by the nodeless Balian-Werthammer state.[69]

Gorkov and Rashba pointed out that the broken inversion symmetry[11] triggers a mixing between spin-singlet and spin-triplet states in the superconducting condensate. With respect to $CePt_3Si$ this would mean that generically the isotropic s-wave state is mixed with the protected spin-triplet state.[66] The superconducting state may then be expressed as

$$\Delta_{\pm}(\vec{k}) = (\psi \pm d|\vec{g}_{\vec{k}}|). \qquad (10)$$

$\Delta_{\pm}$ corresponds to the gap on the two bands split by spin-orbit coupling and ψ is the wave function of the s-wave condensate. As indicated above, $\vec{g}_{\vec{k}}$ vanishes for the C_{4v} symmetry of tetragonal $CePt_3Si$ at $k_x = k_y = 0$. In such a case the superposition of spin-singlet and spin-triplet contributions results in line nodes for $|d| > |\psi|$.[66] It is of importance to note that each of the components separately would *not* produce line nodes.

In a recent study concerning the nuclear magnetic relaxation rate of non-centrosymmetric superconductors, Hayashi et al.[74] proposed such a scenario with a two-component order parameter. The pairing interaction is then characterized by three coupling constants, taking into account interactions within each spin channel and scattering of Cooper pairs between the two channels. Using reasonable temperature dependences of the spin-singlet and the spin-triplet component of the order parameter,[74] this scenario reveals two distinct features: i) slightly below T_c a coherence effect in terms of a Hebel-Slichter peak becomes obvious inferred from coherence effects. ii) Well below T_c the $1/T_1$ relaxation rate behaves proportional to T^3, a power law which is characteristic of line nodes in the gap. The respective function describes the contribution from the density of states.

A comparison of the theoretically obtained results with the experimental $1/T_1$ data reveals fine qualitative agreement, and the two dominating features, i.e., the peak below T_c and the T^3 dependence are well reproduced. This would microscopically corroborate that the superconducting order parameter consists of two components, the spin-singlet (s-wave) and a spin triplet (p-wave) component.

An alternative explanation was put forward by Fujimoto,[75] incorporating the AFM ordered state below about 2.2 K. Fujimoto pointed out that in the triplet-pairing dominated case, the emergence of nodal excitations, or, conversely, the suppression of the SC gap due to the coupling with the AFM order occurs only when the magnetic moment orthogonal to the spin of triplet Cooper pairs exists, which disturbs the formation of the triplet pair.

The Knight shifts K for fields in the basal plane and

along the $\vec{c}$-axis are shown in Fig. 14(a) and (b), respectively for fields of 2 T. These data demonstrate that both components do not change distinctly when the system moves through the superconducting transition temperature. A theoretical treatment of the spin susceptibility, corresponding to the experimental Knight shift, was carried out by Frigeri et al.[76] for the case that the spin degeneracy of the conduction electrons is lifted by the antisymmetric spin-orbit coupling owing to the absence of inversion symmetry. The basic results of these model calculations are: i) In the case of spin-singlet components of the superconducting order parameter the susceptibilities $\chi_{\parallel}$ and $\chi_{\perp}$ both decrease, but keep finite for finite values of the spin-orbit interaction constant α. For $\alpha \to 0$, both components vanish, as in the case of ordinary BCS superconductors, and $\chi(T)$ follows the Yoshida function. The susceptibility becomes stronger suppressed in basal plane than along the $\vec{c}$-axis. ii) For a spin-triplet state with $\vec{d}(\vec{k}) \parallel \vec{g}_{\vec{k}}$, $\chi_{\parallel}$ does not change as the system passes through the superconducting transition temperature. The perpendicular component $\chi_{\perp}$, however, decreases to half of its value at T_c. Moreover, the susceptibility is independent of the spin-orbit interaction strength.

These model calculations in conjunction with the present experimental Knight shift data point at the fact that the spin-triplet component contributes with a substantial fraction to the superconducting condensate in $CePt_3Si$. The observation that the Knight shift even in the basal plane is almost temperature independent, is yet misunderstood. There are hints that impurity scattering may be responsible for the strong increase of $\chi_{\perp}$ in the superconducting temperature range.[77] Very recently, correlation effects have been incorporated by Fujimoto.[78] His model calculations revealed $\chi_{\perp}(T = 0)/\chi_{\perp}(T = T_c) \to 1$ for large values of U/W, where U is the Coulomb correlation energy and W is an average bandwidth.

5. Phase diagram

The preliminary phase diagram, shown in Fig. 15, is compiled from pressure and substitution dependent studies of the electrical resistivity and the specific heat of $CePt_3Si$.[50,56,57] Substitution was done by exchanging Si/Ge. In the most simplest approximation, this isoelectronic process is responsible only for an enlargement of the crystalline unit cell, thus increases the phase space in opposite to the pressure dependent studies.

In order to compare both pressure and volume, a bulk modulus of typical intermetallic compounds, i.e., $B_0 = 1000$ kbar is assumed. Larger or smaller values of B_0 would only compress or stretch the various features. The volume dependence of the characteristic temperatures of the system, i.e, T_N and T_c are then plotted as a function of the reduced volume, V/V_0, where V_0 refers to the volume of $CePt_3Si$ at ambient pressure. Pressure related data correspond to $V/V_0 < 1$, while the Si/Ge substitution follows for $V/V_0 > 1$.

The most important features derived upon the application of pressure are i) the suppression of long range magnetic order with a critical pressure $p_{cr}^{AFM} \approx 6$ to 8 kbar and of the superconducting transition temperature with $p_{cr}^{T_c} \approx 14$ to 16 kbar.[56,57] On the other hand, the Si/Ge substitution causes an increase of the magnetic ordering temperature as well as a decrease of the onset of superconductivity. The increasing unit cell volume derived on the Si/Ge substitution releases pressure from the Ce ion; as a consequence, there is a loss of hybridisation and the $4f^1$ electronic configuration becomes more localised, thus magnetism is stabilised. The strengthening of magnetic order may be the reason why the superconducting transition temperature becomes suppressed in the left part of the phase diagram. Additionally, one has to consider the fact that unconventional superconductivity is very sensitive on pair breaking scattering by non-magnetic impurities as provided by the Si/Ge substitution.

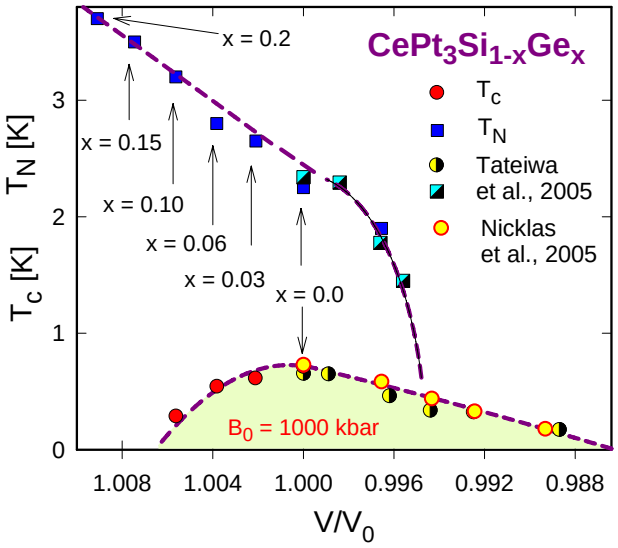

Fig. 15. Phase diagram of $CePt_3(Si_{1-x}Ge_x)$. Data taken from Ref. 50, 56, 57.

The overall superconducting dome is found only in part below the regime with long range magnetic order, while for pressure values $p > 8$ kbar, superconductivity survives in a nonmagnetic environment, supposed to microscopically show distinct different features. The coexistence of long range magnetic order and of superconductivity obvious from Fig. 15 can be interpreted as a hint that magnetic fluctuations are, most likely, a necessary ingredient for binding Cooper pairs, while due to the heavy quasi-particles formed by Kondo interaction in $CePt_3Si$ the retardation effect becomes weak and thus, Cooper pairs mediated by phonons are rather unlikely.

6. Summary

We summarize that non-centrosymmetric $CePt_3Si$ is a heavy fermion SC with $T_c = 0.75$ K that orders magnetically at $T_N = 2.25$ K. Specific heat, NMR and μSR studies indicate that superconductivity and long range magnetic order coexist on a microscopic scale and may be originated by two different sets of electrons. The NMR $1/T_1$ shows unexpected features which were neither found before in conventional nor in heavy fermion SC, indicative of very unusual shapes of the SC order parameter. Unconventional SC is backed also by penetration

depth studies. In fact, the various theoretical scenarios developed for this compound support these conclusions.

Acknowledgment

Work supported by the Austrian FWF P18054.

1) M. Sigrist, in *Lectures on the physics of highly correlated electron systems IX: Ninth Training Course in the Physics of Correlated Electron Systems and High-Tc Superconductors, Salerno, Italy, 4-15 October 2004*, AIP Conference Proceedings 789, ISBN 0-7354-0279-5, editors: A. Avella, F. Mancini, American Institute of Physics, 2005.
2) F. Steglich, J. Aarts, C. D. Bredl, W. Lieke, D. Meschede, W. Franz and H. Schfer: Phys. Rev. Lett. **43**(1979) 1892.
3) N.D. Mathur, F.M. Grosche, S.R. Julian, I.R. Walker, D.M. Freye, R.K.W. Haselwimmer and G.G. Lonzarich: Nature **394** (1998) 39.
4) D. Jaccard, K. Behnia and J. Sierro: Phys. Lett. A **163** (1992) 475.
5) F. M. Grosche, S. R. Julien, N. D. Mathur and G. G. Lonzarich: Physica B **224** (1996) 50.
6) R. Movshovich, T. Graf, D. Mandrus, J. D. Thompson, J. L. Smith and Z. Fisk: Phys. Rev. B **53** (1996) 8241.
7) C. Petrovic, R. Movshovich, M. Jaime, P.G. Pagliuso, M.F. Hundley, J. L. Sarrao, Z. Fisk and J.D. Thompson: Europhys. Lett. **53** (2001) 354.
8) C. Petrovic, P.G. Pagliuso, M.F. Hundley, R. Movshovich, J.L. Sarrao, J.D. Thompson, Z. Fisk and P. Monthoux: J. Phys.: Cond. Mat. **13** (2001) L337.
9) H. Hegger, C. Petrovic, E. G. Moshopoulou, M. F. Hundley, J. L. Sarrao, Z. Fisk and J. D. Thompson: Phys. Rev. Lett. **84** (2000) 4986.
10) P.W. Anderson: *Phys. Rev.* B **30** (1984) 4000.
11) L.P. Gor'kov and E.I. Rashba: *Phys. Rev. Lett.* **87** (2001) 037004.
12) C. Krupka, A. L. Giorgi, N. H. Krikorian and E. G. Szklarz: *J. Less Common Met.* **19** (1969) 113.
13) A. L. Giorgi, E. G. Sklarz, N. H. Krikorian and M. C. Krupka: *J. Less Common Met.* **2** (1970) 131.
14) G. Amano, S. Akutagawa, T. Muranaka, Y. Zenitani and J. Akimitsu: *J. Phys. Soc. Jpn.* **73** (2004) 530.
15) M. Hanawa, Y. Muraoka, T. Tayama, T. Sakakibara, J. Yamaura and Z. Hiroi: *Phys. Rev. Lett.* **87** (2001) 187001.
16) H. Sakai, K. Yoshimura, H. Ohno, H. Kato, S. Kambe, R.E. Walstedt, T.D. Matsuda, Y. Haga and Y. Onuki: *J. Phys.: Cond. Mat.* **13** (2001) L785.
17) K. Togano, P. Badica, Y. Nakamori, S. Orimo, H. Takeya and K. Hirata: Phys. Rev. Lett. **93** (2004) 247004.
18) P. Badica, T. Kondo and K. Togano: J. Phys. Soc. Jpn. **74** (2005) 1014.
19) M. Nishiyama, Y. Inada and G.-q. Zheng: Phys. Rev. B **71** (2005) 220505(R).
20) H. Q. Yuan, D. F. Agterberg, N. Hayashi, P. Badica, D. Vandervelde, K. Togano, M. Sigrist and M. B. Salamon: Phys. Rev. Lett. **97** (2006) 017006.
21) E.R. Domb and W.R. Johnson: J. low Temp. Phys. **33** (1978) 29.
22) V. M. Edelstein: Phys. Rev. B **67** (2003) 020505, and ref. cited therein.
23) E. Bauer, G. Hilscher, H. Michor, Ch. Paul, E.W. Scheidt, A. Gribanov, Yu.Seropegin, H. Noel, M. Sigrist and P. Rogl: *Phys. Rev. Lett.* **92** (2004) 027003.
24) T. Akazawa, H. Hidaka, T. Fujiwara, T. C. Kobayashi, E. Yamamoto, Y. Haga, R. Settai and Y. Onuki: *J. Phys.: Cond. Mat.* **16** (2004) L29.
25) N. Kimura, K. Ito, K. Saitoh, Y. Umeda, H. Aoki and T. Terashima: *Phys. Rev. Lett.* **95** (2005) 247004.
26) I. Sugitani, Y. Okuda, H, Shishido, T. Yamada, A. Thamizhavel, E. Yamamoto, T. D. Matsuda, Y. Haga, T. Takeuchi, R. Settai and Y. Onuki: J. Phys. Soc. Japan **75** (2006) 043703.
27) K. Izawa, Y. Kasahara, Y. Matsuda, K. Behnia, T. Yasuda, R. Settai and Y. Onuki: *Phys. Rev. Lett.* **94** (2005) 197002.
28) I. Bonalde W. Brämer-Escamilla and E. Bauer: *Phys. Rev. Lett.* **94** (2005) 207002.
29) T. Takeuchi, M. Tsujin, T. Yasuda, S. Hashimotto, R. Settai, Y. Onuki, J. Magn. Mag. Mat., in press.
30) A.V. Gribanov, Y.D. Seropegin, A.I. Tursina, O.I. Bodak, P. Rogl and H. Noel: J Alloys and Compounds **383** (2004) 286.
31) A.I. Tursina, A.V. Gribanov, H. Noel, P. Rogl, Y.D. Seropegin and O.I. Bodakd J Alloys and Compounds **383** (2004) 239.
32) O. Sologub, J.R. Hester, P.S. Salamakha, E. Leroy and C. Godart, J. Alloys Compounds **337** (2002) 10.
33) E.W. Scheidt, F. Mayr, G. Eickerling, P. Rogl, E. Bauer: J. Phys.: Cond. Mat. **17** (2005) L121.
34) J.S. Kim, D.J. Mixson, D.J. Burnette, T. Jones, P. Kumar, B. Andraka, G.R. Stewart, V. Craciun, W. Acree, H.Q. Yuan, D. Vandervelde and M.B. Salamon: Phys. Rev. B **71** (2005) 212505.
35) K. Nakatsuji, A. Sumiyama1, Y. Oda, T. Yasuda, R. Settai and Y. Onuki: J. Phys. Soc. Japan **75**, (2006) 084717.
36) G. Motoyama, S. Yamamoto, H. Takezoe, Y. Oda, K. Ueda and T. Kohara: J. Phys. Soc. Japan **75** (2006) 013706.
37) M. Ishikawa, S. Yamashita, Y. Nakazawa, N. Wada and N. Takeda: J. Phys.: Condens. Matter **17** (2005) L231.
38) R. Feyerherm, A. Amato, C. Geibel, F. N. Gygax, P. Hellmann, R. H. Heffner, D. E. MacLaughlin, R. Mller-Reisener, G. J. Nieuwenhuys, A. Schenck and F. Steglich: Phys. Rev. B **56** (1997) 699.
39) R. Modler, M. Lang, C. Geibel, C. Schank and R. Mueller-Reisener: Physica B **206 - 207** (1995) 586.
40) M. Ishikawa, N. Takeda, P. Ahmet, Y. Karaki and H. Ishimoto: J. Phys.: Condens. Matter **13** (2001) L25-L31.
41) M. Giovannini, H. Michor, E. Bauer, G. Hilscher, P. Rogl, T. Bonelli, F. Fauth, P. Fischer, T. Herrmannsdrfer, L. Keller, W. Sikora, A. Saccone and R. Ferro: Phys. Rev. B **61** (2000) 4044.
42) E. Royanian: PhD-thesis, Vienna University of Technology, in preparation.
43) J.G. Sereni, C. Geibel, M.G-Berisso, P. Hellmann, O. Trovarelli and F. Steglich: Physica B **230-232** (1997) 580.
44) D.T. Adroja et al., to be published.
45) M. A. Continentino, S. N. de Medeiros, M. T. D. Orlando, M. B. Fontes and E. M. Baggio-Saitovitch: Phys. Rev. B **64** (2001) 012404.
46) N. Metoki, N.Metoki, K.Kaneko, T.D.Matsuda, A.Galatanu, T.Takeuchi, S.Hashimoto, T.Ueda, R.Settai, Y.Onuki and N.Bernhoeft: *J. Phys.: Cond. Mat.* **16** (2004) L207.
47) H.U. Desgranges and K.D. Schotte: Phys. Lett. A **91** (1982) 240.
48) M. Besnus, A. Braghta N. Hamdaoui and A. Meyer: J. Magn. Magn. Mat. **104 - 107** (1992) 1385.
49) D. Cornut and B. Coqblin: Phys. Rev. B **5** (1972) 4541.
50) E. Bauer, G. Hilscher, H. Michor, M. Sieberer, E.W. Scheidt, A. Gribanov, Yu. Seropegin, P. Rogl, A. Amato, W.Y. Song, J.-G. Park, D.T. Adroja, M. Nicklas, G. Sparn, M. Yogi and Y. Kitaoka: *Physica* B **359-361** (2005) 360.
51) J.G Park et al., to be published (2006).
52) P. Schlottmann: Z. Physik B **51** (1983) 223.
53) N. Kawakami and S. Okiji: J. Phys. Soc. Jpn. **55** (1986) 2114.
54) T. Graf, J. M. Lawrence, M. F. Hundley, J. D. Thompson, A. Lacerda, E. Haanappel, M. S. Torikachvili, Z. Fisk and P. C. Canfield: Phys. Rev. B **51** (1995) 15053.
55) T. Graf, R. Movshovich, J. D. Thompson, Z. Fisk and P. C. Canfield: Phys. Rev. B **52** (1995) 3099.
56) M. Nicklas, G. Sparn, R. Lackner, E. Bauer and F. Steglich: Physica B **359 - 361** (2005) 386.
57) N. Tateiwa, Y. Haga, T.D. Matsuda, S. Ikeda, T. Yasuda, T. Takeuchi, R. Settai and Y. Onuki: J. Phys. Soc Jap. **74** (2005) 1903.
58) A.P. Mackenzie and Y. Maeno: Rev. Mod. Phys. **75** (2003) 657.
59) A. Amato, E. Bauer and C. Baines: Phys. Rev. B **71** (2005) 092501.
60) T. Yasuda, H. Shishido, T. Ueda, S. Hashimoto, R. Settai, T.

Takeuchi, T. D. Matsuda, Y. Haga and Y. Onuki: J. Phys. Soc. Jpn. **73** (2004) 1657.
61) K.V. Samokhin, E.S.Zijlstra and S.K.Bose: Phys. Rev. B **69** (2004) 094514.
62) S. Hashimoto, T. Yasuda, T. Kubo, H. Shishido, T. Ueda, R. Settai, T.D. Matsuda, Y. Haga, H. Harima and Y. Onuki: J. Phys.: Condens. Matter **16** (2004) L287.
63) P.A. Frigeri, D.F.Agterberg, A.Koga and M.Sigrist: Phys. Rev. Lett. **92** (2004) 097001.
64) L.N. Bulaevski A.A. Guseinov and A.I. Rusinov: *Sov. Phys. JETP* **44** (1976) 1243.
65) R. P. Kaur, D. F. Agterberg and M. Sigrist: Phys. Rev. Lett. **94** (2005) 13702.
66) D.F. Agterberg P.A. Frigeri, R.P. Kaur, A. Koga and M. Sigrist: Physica B **378380** (2006) 351.
67) I. Bonalde, W. Brämer-Escamilla, C. Rojas, Y. Haga, E. Bauer, T. Yasuda and Y. Onuki: Proc. of the 8th International Conference on Materials and Mechanisms of Superconductivity and High Temperature Superconductors, Dresden, Germany, 2006.
68) N. Hayashi, K. Wakabayashi, P. A. Frigeri and M. Sigrist, Phys. Rev. B **73** (2006) 024504.
69) M. Yogi, Y. Kitaoka, S. Hashimoto, T. Yasuda, R. Settai, T.D. Matsuda, Y. Haga, Y. Onuki, P. Rogl and E. Bauer: Phys. Rev. Lett. **93** (2004) 027003.
70) M. Yogi, H. Mukuda, Y. Kitaoka, S. Hashimoto, T. Yasuda, R. Settai, T.D. Matsuda, Y. Haga, Y. Onuki, P. Rogl and E. Bauer: J. Phys. Soc. Japan **75** (2006) 013709.
71) L.C.Hebel and C.P. Slichter: Phys. Rev. **107** (1957) 901.
72) H. Tou, Y. Kitaoka, K. Asayama, C. Geibel, C. Schank and F. Steglich: J. Phys. Soc. Jpn. **64** (2003) 725.
73) R. Balian and N. R. Werthamer, Phys. Rev. **131** (1963) 1553.
74) Hayashi et al., cond-mat/0504176.
75) S. Fujimoto: J. Phys. Soc. Japan **75** (2006) 083704.
76) P.A. Frigeri, D.F. Agterberg and M. Sigrist: New J. Phys. **6** (2004) 115.
77) private communication.
78) S. Fujimoto, cond-mat/0605290.

View publication stats